

Research article

# Prionogenicity of vimentin surmised from the sequelog of anti-idiotypic antibodies toward the paratope of malignant-associated autologous anti-vimentin antibody, CLN-IgG (Pritumumab)

Albert V. Hugwil\*<sup>1</sup>, Mark C. Glassy<sup>1,2</sup>

<sup>1</sup> HIHIMSA Foundation, Oceanside, California 92054, USA

<sup>2</sup> Translational and Neuro-oncology Laboratory, UCSD Moores Cancer Center, La Jolla California, USA

\*Corresponding author: Albert V. Hugwil, 1.HIHIMSA Foundation, Oceanside, California USA, E-mail: alhugwil@gmail.com

Received: June 02, 2018; Accepted: June 22, 2018; Published: June 24, 2018

## Abstract

CLN-IgG (Pritumumab) is the natural human monoclonal antibody recognizing the altered-vimentin expressed on ectosomes of malignant cells. Comparative analysis of the sequelogous complementarity determining regions of the five anti-idiotypic antibodies to the paratope of CLN-IgG implied that the core epitope found in vimentin possessed prionogenic potential to form coacervates tending to amyloidosis, which are called vimentin prionogenic idiotope determining amino acids motif (*vipidam*). Sets of the sequelog of *vipidam* were found in countless prions and prion-like proteins. CLN-IgG carries over the sequelog of *vipidam* in its paratope, which was found not only in 14-3-3 proteins but also in  $\alpha$ -synuclein. The effectiveness of Pritumumab on brain tumor regression was inferred by its intervention on vimentin prionogenesis via a prion silencing mechanism attributed to the chaperonic antibody like CLN-IgG (Pritumumab).

Keywords: Human monoclonal antibody Pritumumab, Vimentin Epitope, Prions, Amyloid, Brain Tumor, Idiotypic Antibody Networks

## Introduction

Prionogenicity in regard to prion diseases evaluated with the expression of prions (PrP), prion-like proteins (PrLP) and proteins with prion propensity (PrPP) has emerged recently in conjunction with inflammation and tumorigenesis [1, 2] and not solely with neurodegenerative diseases [3, 4]. Furthermore prion's neuroprotective function has shed light on neural networks [5]. On the other hand EMT (epithelial-mesenchymal transition) and the counter phenomenon MET (mesenchymal-epithelial transition) is a cue for tumorigenesis provoking malignant traits such as metastasis, invasion, anti-apoptosis, and chemotherapy resistant [6]. Vimentin expression is a hallmark of EMT/MET [7]. Recently the role of prion-like ribonucleoproteins on the splicing of RNA in stem cells was found during EMT [8]. Regulation of

cancer stem cells by epigenetic reprogramming is one of the most modern approaches in the field of cancer therapy [9]. In 1982 a human monoclonal antibody CLN-IgG recognizing autologous cervical carcinoma was generated [10] by use of human x human hybridoma technology with cervical cancer lymphnode lymphocytes [11], and the hybridoma was named CLN-SUZ-H11.

Early on a tumor-associated antigen TA226 was identified by use of this natural human monoclonal antibody CLN-IgG (INN: Pritumumab) [12]. The epitope of TA226 resided on 79 amino acids (aa) in Coil2B of vimentin as a common antigen of the malignant cell which was known as the vimentin-epitope79 [13]. At the cell cycle G2/M, TA226 is expressed on the plasma membrane of the ectosome protrusions called ecto-domain vimentin (EDV)

[14]. In the last 30 years, the efficacy of repetitive administration of Pritumumab has been evaluated toward brain tumor patients and resulted more than 28% of complete and partial remission, and more than 70% including moderate remissions and stable response with the dose of 1 mg CLN-IgG per twice a week [15]. The true mechanism how Pritumumab showed such remarkable responses were unclear in the antigen specific immunotherapy against brain tumors. However during the course of clinical trials of Pritumumab, the augmentation of anti-anti-idiotypic antibody (Ab3) to CLN-IgG (Ab1) was found in the serum of the patients who responded well to Pritumumab therapy and Ab3 showed aperiodic circaseptan rhythms in the good responders [16]. Here in this report we investigated the mechanisms of Ab3 augmentation underlying idiotypic antibody networks in idiotope image transmission (IIT) found in the good responders with Pritumumab therapy through the comparative analysis of the complementarity determining regions (CDRs) of the paratactic idiotypic antibodies toward CLN-IgG. In summary we propose a mechanism of tumor regression in the patient who received Pritumumab therapy might be evoked by intervention of chaperonic CLN-IgG against the prionogenic vimentin epitope that is termed with *vipidam* (vimentin prionogenic idiotope determining amino acids motif).

## Materials and Methods

### Determination of amino acid sequences of CLN-IgG:

To isolate total RNA, the human x human hybridoma cell line CLNH11 (ATCC-HB8307) with  $10^9$  cells were centrifugally washed (1,000 x g) with saline and the cell pellets were homogenized in 20 ml of 5M guanidinium thiocyanate with 8% 2-mercaptoethanol. The homogenate was mixed in 7.5 ml ethanol-pre cooled at  $-20^{\circ}\text{C}$  in polypropylene test tube following by immediate centrifugation 10,000 x g for 5 min. To the resulting precipitate 10 ml of cold 5M guanidinium thiocyanate was added with 8% of 2-mercaptoethanol and then homogenized by adding 0.25 ml of 1M acetic acid and 7.5 ml of cold ethanol and left over night at  $-20^{\circ}\text{C}$ . The precipitate obtained by centrifugation at 10,000 x g 10 min was resolved in 10 ml 6 M guanidinium chloride followed by adding 0.25 ml 1M acetic acid and 5 ml cold ethanol and then stored over 3 hr at  $-20^{\circ}\text{C}$ . The precipitate obtained by centrifugation at 10,000 x g 10 min was resolved in 5 ml of 6M guanidine chloride following by adding 0.125 ml 1 M acetic acid and 2.5 ml of cold ethanol and then stored again over 3 hr at  $-20^{\circ}\text{C}$ . The precipitate obtained by centrifugation at 10,000 xg for 10 min was resolved in 5 ml sterilized pure water. This was followed by adding 0.5 ml 2M sodium chloride and 12.5 ml of cold ethanol and then stored at  $-20^{\circ}\text{C}$  as the total RNA fraction.

For the preparation of poly-A-RNA by the method of Chirgwin, the total RNA from CLNH11 (9 mg) was

resolved in the endotoxin free pure water resulting in 2.5 mg/ml RNA solution. The RNA solution was treated with  $100^{\circ}\text{C}$  for 5 min and then cooled in ice followed by adding 5M LiCl, 10% SDS and 1M Tris-HCl (pH7.4) to obtain the final concentration of 0.5M, 0.2% and 10 mM, respectively (LST buffer). This RNA solution was subjected to oligo(dT) cellulose column-equilibrated with LST buffer. The oligo(dT) cellulose column was washed with 10 times volume of LST buffer. Poly-A-RNA fraction was eluted by washing buffer with 10 mM Tris-HCl (pH7.4) and treated with  $100^{\circ}\text{C}$  for 5 min. The oligo(dT) cellulose chromatography was performed once again with the new column. The eluted poly-A-RNA was precipitated by adding 2.5 times (v/v) of ethanol and 1/10 times (v/v) of 2M sodium acetate and then centrifuged with 10,000 x g for 5 min. The purified poly-A-RNA was resolved in sterilized pure water at a concentration of  $2\mu\text{g}/\mu\text{l}$  at  $-70^{\circ}\text{C}$  and stored until needed.

The preparation of cDNA library from CLNH11 was performed by use of the Kit for cDNA synthesis (Amersham, Sweden). The purified poly-A-RNA ( $4\mu\text{g}$ ) of CLNH11 was used in the  $3.2\mu\text{g}$  cDNA synthesis. This cDNA was treated with EcoRI methylase and then both ends of the cDNA were ligated with EcoRI linkers. After the EcoRI digestion, cDNA possessing EcoRI sites was purified by use of Amersham column. The obtained cDNA (100 ng) was linked into  $1\mu\text{g}$   $\lambda\text{gt}$  vector (Transgene, USA) and cloned by use of packaging Kit (GIGA-PACK GOLD, Stratagene, USA). CLNH11 cDNA library had  $7.8 \times 10^6$  pfu/ $\mu\text{g}$  DNA).

For the partial sequence determination of CLN-IgG ( $\gamma$  1-heavy and  $\kappa$ -light chains), which was purified from the human x human hybridoma CLNH11 by use of ion-exchange chromatography (SP sepharose fastflow, Amersham-Pharmacia, Japan), protein A-coupled Sepharose affinity chromatography (IPA400, Repligen USA) and gel filtration (Sephacryl S-300HR, Amersham-Pharmacia, Japan) resulting in over 99% purity. The purified CLN-IgG was alkylated under reducing conditions. The heavy chains and light chains were fractionated by gel filtration and then the N-terminal amino acid sequence ( $\sim 30$  aa) of the heavy chain and light chain were determined by use of several protein sequencers (Applied Biosystems, USA). The heavy chain was especially digested by BrCN at Met sites and then the resulting fragments were purified by reverse-phase HPLC (Waters, USA). The collected fragments were also determined by a protein sequencer.

For the preparation of a probe for CLN-IgG heavy chain DNA sequence determination, homologous amino acid sequence (sequellog) was investigated in the NBRF-PDB (National Biomedical Research Foundation Protein Data Base) corresponding to the N-terminal amino acid sequences of CLN-IgG $\gamma$ 1. As a result the human immunoglobulin germ line VH26 (Entry name:

H3HU26, Accession no. A02047) was identified as the highest sequelog. Therefore the DNA primer No.1 was synthesized (SHIMAZU DNA synthesizer, Japan) having the DNA sequence homologous the 30-nucleotides of N-terminus of 10-aa of VH26 (ID:HSIGHAU, Accession no. M17747) in EMBL-PDB. Also the DNA primer No.2 was synthesized to have the DNA sequence homologous to the 30-nucleotides of C-terminus 10-aa of VH26 (ID:HSIGGCC4, Accession no. J00228) in EMBL-PDB. Using these primer No.1 and No.2, PCR (PerkinElmer, USA) was performed to amplify cDNA of CLNH11 (4 ng) resulting in the DNA fragment with ~660 bp (PCR $\gamma$ C3). This fragment contained immunoglobulin IgG VH and  $\gamma$  CH1. PCR $\gamma$ C3 was biotinylated as a probe for the determination of CLN-IgG  $\gamma$ 1-chain. For the preparation of probe for CLN-IgG light chain DNA sequence determination, the homologous amino acid sequence (sequelog) was investigated in the NBRF-PDB corresponding to the N-terminal amino acid sequences of CLN-IgG  $\kappa$ . As a result this showed human immunoglobulin from Daudi cells had the highest homology (Entry name:K1HUDI, Accession no. A01884). Therefore the DNA primer No.3 was synthesized having the DNA sequence homology 30-nucleotides of N-terminus 10-aa of Daudi (ID:HSVK02, Accession no. X00966) in EMBL-PDB. Besides the DNA primer No.4 was synthesized having the DNA sequence homologous to 30-nucleotides of C-terminus 10-aa of Daudi (ID:HSIGK1, Accession no. V00557) in EMBL-PDB. Using these primer No.3 and No.4, PCR was performed to amplify cDNA of CLNH11 (4 ng) resulting in the DNA fragment with ~660 bp (PCR $\kappa$ A4). This fragment contained immunoglobulin IgG VL and  $\kappa$  CL1. PCR $\kappa$ A4 was biotinylated and used as the probe for the determination of CLN-IgG  $\kappa$ -chain. For the screening of CLN-IgG heavy chain cDNA, plaque hybridization was performed on  $\lambda$ gt10 library by use of biotinylated probe PCR $\gamma$ C3 resulting in 13 positive clones. A clone having the full length of CLN-IgG $\gamma$ 1 ~1.6 K-bp was named  $\lambda$ CLN-G111. For the screening of CLN-IgG light chain cDNA, plaque hybridization was performed by use of biotinylated probe PCR $\kappa$  A4 resulting in 27 positive clones. A clone having the full length of CLN-IgG $\kappa$  ~1.0 K-bp was named  $\lambda$ CLN-K411.

For the full amino acid sequence of CLN-IgG, the clones of  $\lambda$ CLN-G111, and  $\lambda$ CLN-K411 were subjected to the determination of their DNA sequences. Each EcoRI fragment was re-cloned into the phagemid Bluescript SK+ E.Coli XL1-Blue followed by the infection of helper phage R408 to obtain single strand DNA corresponding to CLN-IgG $\gamma$ 1 and CLN-IgG $\kappa$ . DNA sequence of heavy chain and light chain were determined by use of the Sanger method and the Plex luminescence Kit (Millipore, Japan) following by the automated DNA sequencer (SHIMAZU, Japan) and then the full length aa sequence was deduced for CLN-IgG VL + CL1 and VH + CH1 + CH2 + CH3.

CLN-IgG had glycosylation site in CH2 and possessed a human type poly-saccharide chain as well.

### Determination of amino acid sequences of idiotypic antibody (Idio-Ab)

The murine hybridomas termed with Idio-33, 20, 17, 3 and 27 (all isotypes were  $\gamma$ 1-heavy chain and  $\kappa$ -light chain) secreting anti-paratactic murine antibody toward CLN-IgG were generated by use of mouse hybridoma technology mentioned previously [17]. The key point was to immunize new born mice with irrelevant human IgG with relatively high dosage (100 $\mu$ g/shot) at one day the mice to be tolerated toward the secondary immunization with Fab fragment of CLN-IgG. The amino acid sequence of each murine monoclonal antibody was determined from each murine hybridoma clone. The specified procedures mentioned above was used for the determination of the Idio-Ab's amino acid sequences.

### Three-dimensional analysis of the paratope of CLN-IgG and the epitopes of Idio-Ab

The three-dimensional molecular models of CLN-IgG and Idio-3 were configured by use of BIOCES/NEC program [17]. In short the homologous proteins in the amino acid sequence of the antibodies were searched for PDB and we selected the human anti-HIV gp41 antibody 3D6 Fab fragment for CLN-IgG and the anti-hen lysozyme antibody D11.15 Fv fragment for Idio-3 as the reference protein. The models were constructed by referring to information from the spalog proteins. The models were refined by calculations using the Monte Carlo method and molecular mechanics. The computer graphics were used to design the space-filling model and curvature model for CLN-IgG Fv and Idio-3 Fv mirrored the structure of the CLN-IgG paratope, which corresponded to the topographical epitope posture that was composed by 6 CDRs of Idio-3 Ab.

### Immunohistochemical staining with CLN-IgG

Immunoperoxidase staining was performed with clinical grade CLN-IgG (INN: Pritumumab) to the human brain tumor specimens as reported previously [12]. The key point was on the usage of freshly obtained frozen sections. The ordinal formaldehyde embedded samples sometime resulted in negative staining with CLN-IgG. Tissue sections were prepared before the clinical trial of Pritumumab (CLN-IgG) for immunohistochemical (IHC) staining with CLN-IgG and passed through the internal reviews of the ethical committee of neurosurgery and the written informed consent was prepared for each case of Pritumumab antigen specific immunotherapy to the brain tumors.

## Results

### Definition of the idiotope, paratope and epitope of CLN-IgG and Idio-Ab

Vimentin was purified by use of affinity chromatography coupled with CLN-IgG and showed the molecular profile p226K in SDS-PAGE (TA226: composed by a-subunit p60K x 2 + b-subunit p53K x 2 = p226K) from the mass-culture of tumor cell lines such as U251MG (glioblastoma), Hela229 (cervical cancer), G361(melanoma), A549 (lung cancer) and Colo205 (colon cancer) as the solid tumor-associated common antigen [12]. The epitope of vimentin was expressed on the special protrusions on the cell membrane during G2/M phase and it was called the vimentin-epitope79 exposing ectosome (VEE) [13,14]. On the other hand anti-CLN-IgG paratope specific idiotypic antibodies were generated by use of murine hybridoma technology. Five murine hybridomas were cloned and each monoclonal Ab was purified and designated with Idio-33, 20, 17, 3 and 27. By using Western blotting with Idio-33, TA34 (p34K) was identified in SDS-PAGE under reducing conditions [13]. Idio-Abs inhibited completely CLN-IgG binding to the target tumor cells with stoichiometrically one-to-one molar ratio showing the  $\beta$ -type counter epitope binding to the complete configuration of the CLN-IgG antigen-combining site [14]. The paratope of the antibody is constituted by 6 CDRs (complementarity determining regions) composing the epitope recognition site in a variable region (VL and VH) of CLN-IgG Ab which configures the posture of the TA34 epitope that was recognized by Idio-Abs [17]. On the contrary the epitope of Idio-Ab possessed the posture of vimentin-epitope79 that was recognized by the paratope of CLN-IgG [13]. Anti-paratactic idiotypic antibody against CLN-IgG (Ab1) paratope is termed anti-idiotypic antibody (Ab2). Anti-paratactic idiotypic antibody against Ab2 paratope is termed anti-anti-idiotypic antibody (Ab3). Likewise CLN-IgG Ab1 administration evoked Ab2→Ab3→Ab4→Ab5→Ab6 propagation like a water droplet making ripple currents according to the concept of Jerne's idiotypic antibody network theory [18]. These sequential idiotope transmissions in idiotypic antibody networks are called Idiotope Image Transmission (IIT) in this report.

### Comparison of aa sequences of variable regions of CLN-IgG and its paratactic idiotypic Abs

The DNA sequences corresponding to CLN-IgG VH+CH1+CH2+CH3 and VL+CL1 were determined by DNA cloning technique and the deduced amino acid (aa) sequences were determined by use of the triplet base codon translation. The antigen binding site consisting of 6 CDRs of CLN-IgG were marked by use of the Kabat definition (Table 1). On the other hand anti-idiotypic antibodies (Idio-Abs) were generated by use of murine hybridoma technology. Five Idio-Abs specific for the paratope of

CLN-IgG were selected through the competition assay of CLN-IgG bindability to the target cells with U251MG human glioblastoma cell line and named in decreasing order of bindability Idio-33>Idio-20>Idio-3>Idio-17>Idio-27 along with the inhibitory activities of CLN-IgG toward the tumor associated antigen TA226 of U251MG. The aa sequence of each Idio-Ab was determined by the same method as the sequence determination used for CLN-IgG. The reasons why we focused on the CLN-IgG VL/VH-CDR1s were that 1) vimentin was purified from U251MG through CLN-IgG coupled Sepharose 4B-affinity chromatography in the chaotropic ionic condition with 2M NaCl + 5M Urea for the denaturation of protein structure, 2) interaction between Idio-Abs and CLN-IgG was also measured in the presence of 2M NaCl + 5M Urea. Therefore the N-terminus adjunct stretched CDR1s of CLN-IgG must contribute to epitope recognition thus we could omit the consideration of steric orientations of the linear polypeptide epitopes, and 3) since CDR2 and CDR3 had a relatively long aa motif and were frequently observed variation of insertion and deletion, the short stretched CDR1 motifs having a pentamer in CLN-IgG VH-CDR1 and a heptamer in VL-CDR1 made it seem feasible to compare the sequelogs toward epitope motifs carried over on Idio-Abs. The critical aa sequence for antibody-antigen/epitope recognition sites including VL-CDR1 and VH-CDR1 of CLN-IgG and Idio-Abs are aligned in Table 1. DISNYLA and NYAMS in VL-CDR1 and VH-CDR1 of CLN-IgG are counter motifs set vis-a-vis and it was described in terms of DISNYLA/NYAMS. In order to get an imaginable configuration of the core epitope in vimentin, the space filling model of the idiotope that consisted of 6 CDRs of Idio-3 was constructed for an example of the topographical posture of the core vimentin-epitope79 found in Coil2B. The idiotope of Idio-3 was discerned mimicking the core of vimentin-epitope79 posturing like a spallog presenting cavernous topographical feature. As a trope of this core epitope, we put the nick-name on this spallog the countenance "*Chagrin*" in this report (Figure1). Since DISNYLA looks like a stretched finger on CLN-IgG VL-CDR1 toward the counter motif of NYAMS, it was speculated that a mimotope of NYAMS should be in Idio-Ab's VH-CDR1. We found a NYWMQ pentamer motif in Idio-33 VH-CDR1, which showed the most reactive paratactic idiotypic Ab to CLN-IgG. Strikingly the sequelogous NYQDT was found in the vimentin-epitope79 in Coil2B of vimentin. From the view of tertiary structure of CDRs of Idio-33, DVTTDVA heptamer in VL-CDR1 of Idio-33 was the pair motif of NYWMQ vis-a-vis described with DVTTDVA/NYWMQ. From here on DISNYLA/NYAMS is denoted with DZZZ-ZLA/NYXXX (D: aspartate, L: leucine, A: alanine, N: asparagine, Y: tyrosine, and Z or X: any amino acids, X:

**Table 1.** Alignment of amino acid sequence of CDRs in the variable region of CLN-IgG and its paratactic idiotypic Abs.

CLN-IgG VLCDR1	28	<b>DISNYLA</b>	34	CLN-IgG VHCDR1	31	<b>NYAMS</b>	35	
Idio-33 VLCDR1	KASQ*****	<b>DVTTDVA</b>		Idio-33 VHCDR1		<b>NYWMQ</b>		
Idio-20 VLCDR1	YRASKSVST*	<b>SGYSYMH</b>		Idio-20 VHCDR1		<b>DYYMN</b>		
Idio-17 VLCDR1	YRASKSVST*	<b>SGYSYMH</b>		Idio-17 VHCDR1		<b>SYWMH</b>		
Idio-3 VLCDR1	YRASKSVQLH	<b>LAIVYMH</b>		Idio-3 VHCDR1		<b>SYWMH</b>		
Idio-27 VLCDR1	KASQ*****	<b>DVNTAVA</b>		Idio-27 VLCDR1		<b>DYYMN</b>		
BJ K-CDR1		<b>DINHLYN</b>		BJ $\gamma$ -CDR1		<b>GYAMT</b>		
CLN-IgG VLCDR2	50	<b>AASSLHS</b>	57	CLN-IgG VHCDR2	48	<b>AITP**</b>	<b>SGGSTN</b>	58
Idio-33 VLCDR2		<b>SASYRYY</b>		Idio-33 VHCDR2		<b>AIYP**</b>	<b>GDGDYR</b>	
Idio-20 VLCDR2		<b>LVSNLDS</b>		Idio-20 VHCDR2		<b>FIRNKA</b>	<b>NLYYTD</b>	
Idio-17 VLCDR2		<b>LVSNLDS</b>		Idio-17 VHCDR2		<b>AIYP**</b>	<b>GNSDIS</b>	
Idio-3 VLCDR2		<b>LVSNLDS</b>		Idio-3 VHCDR2		<b>AIYP**</b>	<b>GNSDIS</b>	
Idio-27 VLCDR2		<b>SASYRYY</b>		Idio-27 VLCDR2		<b>FIRNKA</b>	<b>NYYYE</b>	
BJ K-CDR2		<b>DASNLET</b>		BJ $\gamma$ -CDR2		<b>GITRSG</b>	<b>NAIYNA</b>	
CLN-IgG VLCDR3	91	<b>YSTYPIT</b>	98	CLN-IgG VHCDR3	95	<b>VPYRST</b>	<b>WYP*LY</b>	102
Idio-33 VLCDR3		<b>HYSYAWT</b>		Idio-33 VHCDR3		<b>SGYYGS</b>	<b>FVGFAY</b>	
Idio-20 VLCDR3		<b>HIEGAYT</b>		Idio-20 VHCDR3		<b>DRGGRD</b>	<b>W*YFDV</b>	
Idio-17 VLCDR3		<b>HIRGAYT</b>		Idio-17 VHCDR3		<b>EEYDYG</b>	<b>T**LDY</b>	
Idio-3 VLCDR3		<b>HIRVAYT</b>		Idio-3 VHCDR3		<b>EETDYG</b>	<b>T**LDY</b>	
Idio-27 VLCDR3		<b>HYSPLT</b>		Idio-27 VLCDR3		<b>DGFLRR</b>	<b>W*YFDV</b>	
BJ K-CDR3		<b>YDTLPRT</b>		BJ $\gamma$ -CDR3		<b>DSRVA</b>	<b>AALLTD</b>	

preferably glutamine (Q)). NYQXX provided a special interest in regard to prionogenesis because this sequelog frequently appeared in the aa sequence of typical yeast prion proteins such as Sup35, Rnq1, NEW1, and vertebrate amyloidogenic prion-like proteins such as FUS, DDX23 and hnRNP. The salient feature of aa sequence of prionogenic Q/N-rich proteins possessing NYQXX accompanied by GYQXX and SYQXX [19]. Therefore NYQXX found in vimentin-epitope79 could be affecting the prion propensity of vimentin that behaves like a prion seed [20]. Moreover a sequelog of NYAMS was found in the Bence Jones (BJ) immunoglobulin  $\gamma$ -heavy chain VH-CDR1 GYAMT that shows AH amyloidosis [21].

### Alignment of aa in 14-3-3 proteins as a ligand of the vimentin-epitope79

CLN-IgG bindability to the vimentin-epitope79 was completely inhibited by the Idio-Abs at the stoichiometrically one-to-one molar ratio. Therefore all kinds of Idio-Abs are  $\beta$ -type paratactic Abs that possess the mimicry spalog of vimentin-epitope79 in their paratopes. CLN-IgG VL-CDR1 and VH-CDR1 are positioned vis-a-vis that was designated with DISNYLA/NYAMS. Sequelogenous DISNYLA heptamer motif matching DYYRYLA was found in 7 families of 14-3-3 proteins ( $\beta, \gamma, \delta, \epsilon, \zeta, \eta$ , and  $\sigma$ ) and four of seven are presented in their aa alignments (Table 2). Molecular weight of 14-3-3

proteins calculated in SDS-PAGE was p34K (TA34) that was identical in Western blotting with Idio-3 of U251MG cells [17]. On the other hand vimentin having p60K+p53K in SDS-PAGE was purified by use of CLN-IgG coupled affinity chromatography co-purified with TA34 [13]. Since the purification procedure was carried out in a chaotropic ionic condition with 2M NaCl + 5M Urea, 14-3-3 proteins and vimentin-epitope79 must be tightly associated. As it was mentioned above, Idio-Abs possess the spalog of vimentin-epitope79. Idiotype antibody network theory warned that anti-paratactic Idio-Abs blocks CLN-IgG targeting of TA226. Fortunately Idio-Ab (Ab2) in the patient's serum did not hamper Pritumumab bindability to U251MG in vitro (17). So the augmentation of CLN-IgG after Ab2 that was found in the good responders of Pritumumab therapy did not seem to be caused by canonical mechanism of antigen presentation by antigenic Ab2 Idio-Ab's paratope in idiotype antibody networks. On the other hand 14-3-3 proteins are well known as a good biomarker for diagnosis of neurodegenerative diseases such as Creutzfeldt Jakob Disease (CJD) [22, 23]. In the aa alignment of 14-3-3 together with  $\alpha$ -synuclein, all 14-3-3s have the consensus in the divided aa sequence with KXXK (K:lysine) which was found in KTKE repeats in  $\alpha$ -synuclein (Table 2). Thus  $\alpha$ -synuclein and 14-3-3 could have co-evolved during cellular evolution and possess a chaperonic function for the amyloidogenic aggregates [24].

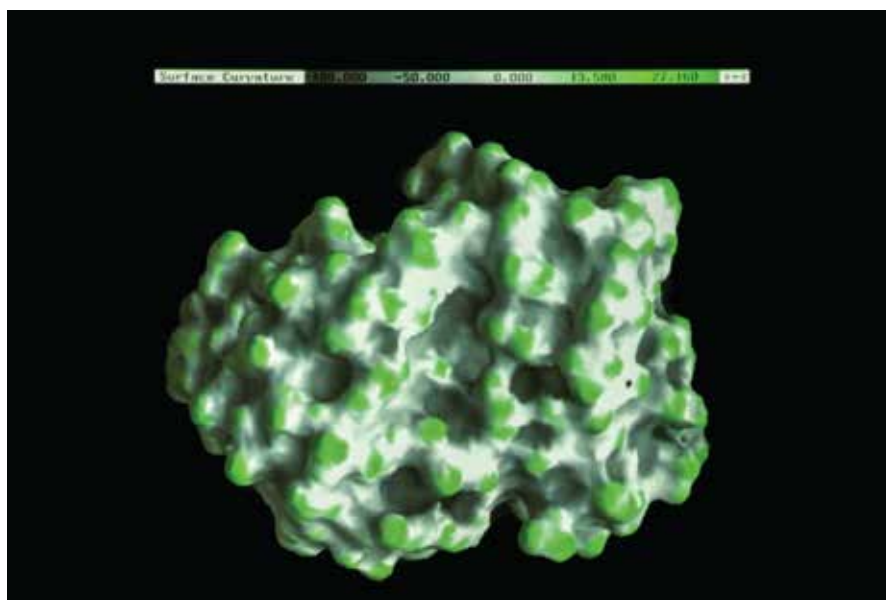


**Figure 1. A surface curvature model for the idiotope of an idiotype antibody against the paratope of CLN-IgG.** Idio-3, a murine monoclonal antibody recognizing p34K protein purified from U251MG glioblastoma cell line, was cloned and its variable domain of the DNA sequence was determined. A space filling model of Idio-3 was constructed by use of BIOSE(NEC) program from the deduced amino acid sequence. The internal image of the epitope binding site composed of 6 CDRs of Idio-3 is represented in this curvature model. The surface configuration is colored gray in order of hydrophobicity ( $\Phi$ ) countering hydrophilicity (green). This surface posture is a perfect match for the counter paratope of CLN-IgG. The vimentin-epitope79 is recognized by the autologous human monoclonal antibody CLN-IgG, thus this topographical posture mimics the core epitope of vimentin-epitope79, which is called *vipidam* in this paper.

**Table 2.** Alignment of amino acid sequence of  $\alpha$ -synuclein and 14-3-3 proteins.

$\alpha$ -syn	1	MDVFMKGL <b>LSKA</b> KEGVV <b>AAE</b> KTQGV <b>AE</b> AAG <b>KTKE</b> GVLYVGS <b>KTKE</b> GVVHG <b>VATV</b>	55
14-3-3 $\zeta$	41	N <b>LLSV</b> A <b>YKNV</b> V <b>GARR</b> SSWRV <b>VSS</b> IE <b>QKTE</b> GAE <b>KKQ</b> Q <b>MAREY</b> <b>REKI</b> ET	89
14-3-3 $\gamma$	42	N <b>LLSV</b> A <b>YKNV</b> V <b>GARR</b> SGWRV <b>ISS</b> IE <b>QKTS</b> ADG <b>NEKK</b> IEMV <b>RAY</b> <b>REKI</b>	90
14-3-3 $\sigma$	41	N <b>LLSV</b> A <b>YKNV</b> V <b>GGQ</b> RAAW <b>VLSS</b> IE <b>QKS</b> NEEG <b>S</b> E <b>EKG</b> PEV <b>REY</b> <b>REKV</b>	89
14-3-3 $\epsilon$	45	N <b>LLSV</b> A <b>YKNV</b> I <b>GARR</b> ASW <b>RIISS</b> IE <b>QKE</b> ETKG <b>AED</b> KL <b>NMIR</b> AY <b>RSQV</b>	92
		Idio-27 VLCDR1 <b>DVNTAVA</b> *** $\Phi$ * $\Phi$ $\Phi$ * $\Phi$ $\Phi$ $\Phi$ * $\Phi$ $\Phi$ $\Phi$ *** $\Phi$ $\Phi$ ***** <b>DYYMN</b>	
$\alpha$ -syn	56	A <b>EKTKE</b> QVT <b>NVGG</b> AV <b>VTGVT</b> A <b>V</b> AQ <b>KTVE</b> GASS <b>IAA</b> AT <b>GFV</b> KKD <b>QLG</b> KE <b>GYQ</b> D <b>YEPE</b>	112
14-3-3 $\zeta$	90	ELR <b>DIC</b> ND <b>VLS</b> LL <b>EKFL</b> IP <b>NAS</b> Q <b>AES</b> RV <b>FYL</b> <b>KMKGD</b> <b>YYR</b> Y <b>LA</b> E <b>V</b> AAG <b>D</b> DK <b>KG</b>	141
14-3-3 $\gamma$	91	E <b>KELE</b> AV <b>CQD</b> V <b>LSLL</b> D <b>NYLI</b> K <b>NC</b> SE <b>TQY</b> ES <b>KV</b> F <b>YL</b> <b>KMKGD</b> <b>YYR</b> Y <b>LA</b> E <b>V</b> AT <b>GE</b>	142
14-3-3 $\sigma$	90	E <b>TELQ</b> GV <b>CDT</b> V <b>LGL</b> LD <b>SHL</b> I <b>KE</b> AG <b>DAE</b> SR <b>VFML</b> <b>KMKGD</b> <b>YYR</b> Y <b>LA</b> E <b>V</b> AT <b>GDDK</b>	141
14-3-3 $\epsilon$	93	E <b>KELR</b> D <b>ICSD</b> I <b>LGV</b> LD <b>KYLY</b> P <b>SSQ</b> T <b>GES</b> K <b>V</b> F <b>Y</b> <b>KMKGD</b> <b>YH</b> R <b>YLA</b> E <b>PAT</b> G <b>NDR</b>	143
		CLN-IgG VLCDR1 <b>DISNYLA</b>	
		<b>(DZZZZLA)</b>	

$\alpha$ -Synuclein is the causative prion found in the amyloid of Parkinson disease (PD) and Alzheimer disease (AD) [25]. 14-3-3 $\epsilon$  was also simultaneously found in the prion amyloid deposits of Gerstmann-Sträusler-Scheinker disease GSS [26]. The respective sequelog of DZZZZLA in Idio-33 DVTTDVA or Idio-27 DVNTAVA was found in  $\alpha$ -synuclein 72TGVTAVA78, moreover it was found in the Bence Jones (BJ) immunoglobulin  $\kappa$ -light chain VL-CDR1 showing a sequelog with DINHYLN in the AL amyloidosis (Table 1) [27]. These sequelogs of DZZZZLA were found in the potential prionogenic 14-3-3 proteins and CLN-IgG, and they may function as the chaperones against prions. In fact association of 14-3-3 with amyloidogenic aggregates were reported regarding Lewy Bodies in PD, Neurofibrillary tangles in AD, mutant Huntingtin in HD, mutant SOD in ALS, so on [28]. Also the spallog mimicking of the mirror image of CLN-IgG VL-VH to the vimentin-epitope79 can be inferred of the potential prionogenicity of the paratope of CLN-IgG.

### The *vipidam* sequence in the vimentin-epitope79 is the surmised core motif for prionogenicity

Since the idiotope of the five Idio-Abs are the perfectly matched counter epitope to the paratope of CLN-IgG, the

surface posture of the Idio-Ab is a spallog mimicking the moiety of vimentin-epitope79. Verification of visible curvature by computer-assisted analysis of anti-paratactic Idio-Ab gave us an internal image of the core of vimentin-epitope79-*Chagrin* (Figure 1). The 16-oligomer aa 346EMEENFAVEAANYQDT361 found in vimentin-epitope79 is termed "*vipivam*" standing for "vimentin prionogenic idiotope determining amino acids motif". This motif was also considered as a "vimentin prionogenic intrinsic disordered amino acids motif" in this report (Table 3A). EMEENFA was considered a variation from DZZZZLA motif when it was compared to aa array of intermediate filament proteins (IFPs) (Table 3-B). Lamin A possesses DLEDSL and this motif has diversified among IFPs. It should be emphasized that *vipidam* includes a stutter motif FAVEAA that is related to the robustness of vimentin filament against mechanical stress [29, 30]. From the aspect of structural mimicry as a spallog, EMEENFA corresponds to DZZZZLA. From here on *vipidam* is denoted with EZ $\Phi$ NX. There is a rudimental constituent of the aa sequence motif regarding coacervate as found in EZ $\Phi$ NX composed by  $\Phi$ : hydrophobic aa that are sandwiched with negatively hydrophilic aa E (E: glutamate preferably E/D) and positively hydrophilic aa

**Table 3.** Amino acid sequence of the prionogenic vipidam in vimentin-epitope79 and its alignment between other intermediate filament proteins.

**Table 3A.** Vimentin Coil2B.

245	QAQIQEQHVQIDVDVSKPDLTAALRDVRRQOYESVAAKNLQEA <u>EWYKSKFADLSEAANRN</u>	305
	E Z Φ Φ N X	
	EZZZZΦΦΦEΦΦNYXXX	
306	NDA <u>L</u> RQAKQESTEYRRQVQSLTCEVDALKGTNESLERQMR <b>EMEENFAVEAANYQDT</b> IGRL	365
	CLN-IgG VL/VH-CDR1 DZZZZLA////NYXXX	
366	<u>Q</u> DEIQNMKEEMARHLREYQDLLNVKMALDIEIATYRKLEGEESRISLPLPNFSSLNRE	425
	S**pS*P	
426	TNLDLPLVDTHSKRRTLLIKTVETRDGQVINETSQHDDLE	466

**Table 3B.** IFPs

Vimentin ( <i>vipidam</i> )	339	<u>LERQMR<b>EMEENFAVEAANYQDT</b>IGRLQ</u> DEIQNMKEEMARHL	380
Peripherin (P41219-1)	335	LLRQLRELEEQ <b>FALEAGGYQ</b> AGAARLEELRQLKEEMARHLR	377
Desmin (P17661)	344	LMRQMR <b>ELED</b> RFAS <b>EASGYQ</b> DNIAARLEEEIRHLKDEMARHL	385
GFAP (P14136-1)	305	LERQMR <b>EQE</b> ERNVRE <b>EAASYQ</b> EALARLEEEGQSLKDEMARHL	346
Lamin-B1(P20700-1)	316	CLERIQ <b>ELED</b> LLAKEKDNSRRLTDKEREMAEIRDQMQQQL	357
Lamin-A (P02545-1)	315	KEAKLRD <b>LED</b> SLARERDTSRLLAEKEREMAE MRARMQQQL	355

The vimentin-epitope79 determined by CLN-IgG and vimentin interactions is indicated with underline. EMEENFAVEAANYQDT is called *vipidam* and denoted by EZΦNX. S\*\*pS\*P is the putative 14-3-3 recognition motif. R may be citrullinated arginine.

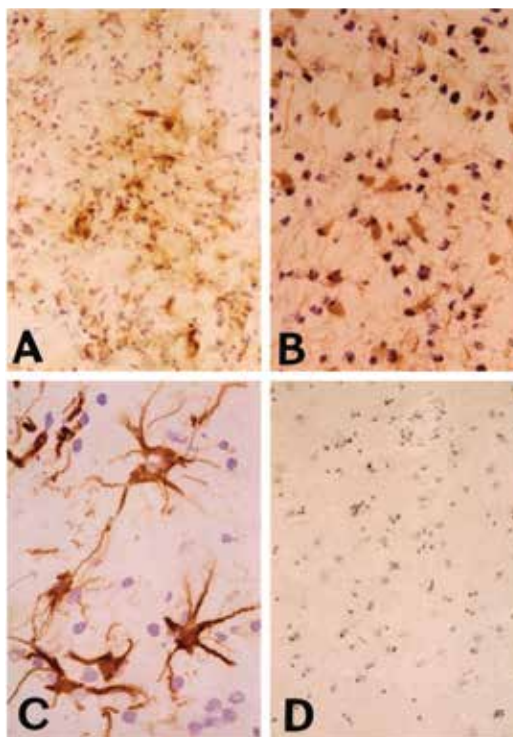
N together with X: any aa preferably Y/Q. The hydrophobic (Φ) aa's are spliced to amphoteric aa's which were also found in CLN-IgG VL/VH-CDR1s.

Coacervates possess a physico-chemical property of membrane-less liquid-droplets that were frequently found in prionogenic polypeptides. Cell-to-cell transmission of prions is one of the most relevant phenomena of prionogenicity. When malignant astrocytoma and glioblastoma were stained with CLN-IgG, tangled fibrils of vimentin were observed around tumor islands indicating anchorage independent tumor growth (Figure 2A), tumor cells were connected with thread-like filaments showing vimentin

networks (Figure 2B) and some tumor cells were connected through the fasciculated vimentin cable (Figure 2C). Although normal brain tissue has also neurons, astrocytes and microglia so on, CLN-IgG did not recognize vimentin in normal brain tissues (Figure 2D). Since EMEENFA seems to be derived from a DZZZZLA pentamer motif, DISNYLA/NYAMS in CLN-IgG VL/VH-CDR1s is interacting with DYYNYLA in 14-3-3. Notwithstanding DYYNYLA in 14-3-3 does not have the paired NYXXX, SYXXX or GYXXX, a single κ-light chain of CLN-IgG interacted with the paratope of Idio-Abs. The idiotope moiety participating paratope-epitope recognition is



**Figure 2. Immunohistochemical staining of glioma patient tissues with the human monoclonal antibody, CLN-IgG.** The purified CLN-IgG was biotinylated and then Bio-CLN-IgG was reacted to various tissue sections from the brain tumor patients before clinical trials with Pritumumab. The positive reaction sites with Bio-CLN-IgG were determined with anti-human IgG coupled with avidin-biotin-peroxidase complex. The reddish brown stains show that vimentin-epitope79 expressing *vipidam* in vimentin Coil2B. Anaplastic astrocytoma (x100) (A), Glioblastoma (x200) (B), Astrocytoma (x400) (C), Normal human fetus brain tissue (x100) (D). Each section was briefly counterstained with hematoxylin to show cell nuclei (purple colored).



termed  $\gamma$ -type idiotope. EZ $\Phi$ NX is a  $\beta$ -type idiotope while  $\gamma$ -type idiotope is denoted EZ $\Phi$  or  $\Phi$ NX.

### EZ $\Phi$ NX motif (*vipidam*) and its derivatives found in prions

Twenty one examples of prions (PrP), prion-like proteins (PrLP) and proteins with prion propensity (PrPP) that possess EZ $\Phi$ NX are listed in Supplementary Tables 1 and 2 from over 100 prionogenic proteins investigated from the UniProtKB data bank. EZ $\Phi$ NX, EZ $\Phi$  or  $\Phi$ NX motifs found in these prionogenic proteins are mostly related to amyloidogenesis in neurodegenerative diseases and cancer. From a comparative analysis of VL/VH-CDRs of CLN-IgG and Idio-Abs together with the aid of computer-assisted epitope image building, the five Idio-Abs listed in this paper should have a tumor antigen epitope image in the *vipidam-Chagrin*. Each Idio-Ab possesses a characteristic aa sequence in each CDR but they have the same spalog *Chagrin* attracted to the paratope of CLN-IgG. We found a sequelog of Idio-3 VL/VH-CDR1 that was in a prion-like protein CPEB4 (cytoplasmic polyadenylation element-binding protein) possessing NQLPHLA/SYQSP (Supplementary Table 1). Furthermore the natural binding of CPEB4 to vimentin was reported in [31,32]. We found the DZZZZLA/NYXXX pair existed in serum amyloid P-component protein (SAP) in von Willebrand disease

(vWD) (Supplementary Table 1). It was reported SAP behaved biphasically in amyloidogenesis of A $\beta$  fibril formation. Anti-amyloidogenicity was evoked by SAP chaperonic activity [33]. EZ $\Phi$ NX found in other prions are listed in the Supplementary Table 2. Each of CJD, Sup-35, TIA1, Rnq1, FUS, NEW1 includes  $\Phi$ NX and each of A $\beta$  amyloid precursor, 14-3-3, HuR includes EZ $\Phi$ . Each  $\alpha$ -Synuclein, Pin2, hnRNP-A1, CPEB4, DDX23 includes EZ $\Phi$ NX. Interestingly isoforms of prionogenic proteins do not possess EZ $\Phi$ NX anymore. Therefore EZ $\Phi$ NX *vipidam* was presumed to be a transient during evolution and it disappeared after the functional purpose was ended leaving a remnant motif of prions. Another interesting pairing in EZ $\Phi$ NX was cross-setting between EZ $\Phi$  and  $\Phi$ NX found in Idio-20 SVSTSGY/DYYMN and Idio-17 SVSTSGY/SYWMH which both have showed the *vipidam* spalog-*Chagrin* to the paratope of CLN-IgG.

### Discussion

In this report, the definition of prion is expanded to include prions (PrP), prion-like proteins (PrLP) and proteins with prion propensity (PrPP) that tends to form amyloid aggregates. The signature of tangles of vimentin and its derivative fibrils were observed associated with amyloid aggregates as seen in neurodegenerative diseases such as Lewy Body in Parkinson Disease (PD) [34],

vimentin-cage in the aggresome of cysticfibrosis transmembrane conductive regulator (CFTR) [35], vimentin-JUNQ inclusion body of intracellular partitioning [36], Huntingtin deposits of Huntington Disease (HD) [37], Amyloid plaques of Alzheimer (AZ) [38], Prions in CJD [26], and so on. The basic structure of vimentin is well described in the literature as having  $\alpha$ -helical structures consisting of coiled-coil domains (*nr*Vimentin). However the topography of vimentin fibrils vary under stress depending on their environmental milieu [39]. A characteristic function of vimentin as opposed other cytoskeletal proteins such as actin and microtubule derives from the stutter region associated with mechanical stress and the stutter motif contributes to information transfer as a molecular seed [29, 30]. In the *vipidam* sequence, 346EMEENFAVEAANYQDT361, the stutter corresponds to FAVEAA that is composed of hyper-hydrophobic amino acids,  $\Phi$ s. So *vipidam* is named EZ $\Phi$ NX in this report. Sequelogs of EZ $\Phi$ NX were found in numerous prionogenic proteins investigated (Supplementary Table1 and 2). Since *vipidam* EZ $\Phi$ NX corresponds to the core epitope of the anti-cancer antibody CLN-IgG (INN: Pritumumab), the affinity of CLN-IgG to *vipidam* was proportional to its tumor suppressive activity [16]. The relevance of Ab-Ag recognition by Pritumumab and TA226 is essential when we think about cancer treatment [14]. If we covet the true cancer cure, epigenetical reprogramming of cancer stem cells is the most crucial modality [40]. In other words recuperation, restoration, and recovery from carcinogenesis depends on how we manage the stresses surrounding us. Prions, 14-3-3 proteins, and vimentin are all stress inducible proteins related to neuronal diseases and tumorigenesis [41, 42, 43].

The *vipidam* recognized by CLN-IgG located in the core vimentin-epitope79 [13] and expressed on the cell surface of the special cell protrusion/buddings called vimentin-exposing ectosome (VEE) [14]. The *vipidam* in the vimentin-epitope79 was recognized by Pritumumab and evoked tumor regression [16]. TA226 was cloned from U251MG and found there were no mutations in the aa sequence compared to the normal version of human vimentin. What kind of mechanism attacks to normal protein epitope resulting in tumor regression from the repetitive administration of autologous human monoclonal antibody, CLN-IgG? The unknown mechanism underlaid augmentation of idiotypic Ab (Ab3) network response in the patient who received Pritumumab immuno-therapy. The good responders showed augmented Pritumumab paratope accompanied by an aperiodic circaseptan rhythm from the repetitive administration of Pritumumab [16]. We hypothesized that it could be accounted for when vimentin-epitope79 evoked Pritumumab self-perpetuation/self-propagation of prions, it acquired the capability of intervention in cell-to-cell communications of tumors. On the other hand vimentin is

a hallmark protein involved in EMT [7]. The mechanism of EMT is complex but closely related to tumor invasion, metastasis, and anti-apoptosis. Furthermore vimentin expression is necessary for stem cell development in embryogenesis [44, 45] and EMT is deeply involved in cancer stem cell maintenance [46]. The 14-3-3s are pivotal for stem cell development [47] and they are abundant in neuronal cells [22]. The 14-3-3s associated with  $\alpha$ -synuclein were found in certain neuronal disordered cells such as CFTR [26] and CJD [35]. The sequelog DZZZZLA pentamer motif in CLN-IgG VL-CDR1 was also in 14-3-3 (DYRYLA) and  $\alpha$ -synuclein (DVTDDVA). So it is natural to wonder about triggering the prionogenic self-perpetuation of CLN-IgG denoted by DISNYLA/NYAMS in its VL/VH-CDR1s. We do not rule out the possibility of a contribution by other CDRs of CLN-IgG for prionogenic aggresome formation because the spallog of vimentin-epitope79 is composed of 6 CDRs. Since vimentin and p34K (TA34) protein were purified in a single step of CLN-IgG coupled affinity chromatography in chaotropic condition in 2M NaCl+5M Urea, Ab-Ag recognition in this case was performed with linear intrinsic disordered protein sequences. From the computer assisted structure analysis of CDRs of CLN-IgG, NYAMS in VH-CDR1 faces to DISNYLA in VL-CDR1 vis-a-vis, so that the DZZZZLA/NYXXX motif in EZ $\Phi$ NX must be effective at promoting prionogenicity in each other. The *vipidam* denoted EZ $\Phi$ NX was found in countless prion and prion-like proteins, especially in Q/N-rich Low Complex Region proteins. The hyper-hydrophobic stutter motif FAVEAA was positioned between EMEENFA (a variant from DZZZZLA) and NYQDT in EZ $\Phi$ NX. EZ $\Phi$ NX leads to formation of coacervate liquid droplets. The topographical flexibility of EZ $\Phi$ NX accounts for the self-antigenicity under severe condition such as oncogenic stresses, thus immune surveillance may evoke chaperone-like activity via CLN-IgG, which is to say as a molecular anvil [48], through the prionogenic Ab production of CLN-IgG to maintain the proteostasis of altered-vimentin.

The physico-chemical characteristics of prions are measured in membrane-less liquid droplets behaving like coacervates [49-51]. They have properties reminiscent of cellular behavior such as fusion, fission, assimilation/dissimilation, self-replication/degradation and horizontal transmission. Particularly intercellular transmission of prions has emerged for tumorigenesis. As seen in Figure 2, *vipidam* were expressed along with vimentin cables between gliomas. In fact the transmission of prions in cell-to-cell communication between astrocytes was reported [52]. Considering the cell-to-cell transmission of *vipidam* through vimentin cables as found in nanotubes (TNT) in malignant mesothelioma [53], the *vipidam* transmission must be crucial for maintenance and propa-

gation of cancer stem cells. If this hypothesis is pertinent, then intervening on *vipidam* should be effective in silencing vimentin prionogenesis. 14-3-3 proteins behave like co-prions with vimentin prionogenesis through DYYRYLA motif. The 14-3-3s are chaperones for phosphorylated proteins [54]. The CLN-IgG's sequence moiety DZZZ-ZLA/NYXXX was found in 14-3-3 proteins and immunoglobulins in AL/AH amyloidosis. So augmentation of the CLN-IgG mimicking antibodies (Ab3) found in brain tumor patients treated with Pritumumab may have been evoked in consonance with vimentin prionogenesis. The augmentation of CLN-IgG (Ab3) showed an aperiodic circaseptan rhythm which we surmised as the assimilation and dissimilation of prionogenic vimentin interacting with chaperonic CLN-IgG (*chap*CLN-IgG). Vimentin also has phosphorylation sites showing the consensus aa sequence R/SXpSXP [55], We propose an additional 14-3-3 binding motif to vimentin through DYNYLA. The 14-3-3 $\gamma$  protein is oncogenic [56], 14-3-3 $\sigma$  is a tumor suppressor (soncogenic) [57] and 14-3-3 $\epsilon$  is an EMT modulator [58]. Therefore sequestration and/or displacement of the relevant 14-3-3 from vimentin-associated aggresomes could be attained by the dynamics of the coacervate *vipidam* inducible vimentin-cage structures [59] that stabilize the specific 14-3-3 needed for proteostasis. By means of the augmented chaperonic paratactic idiotypic CLN-IgG Ab3 contributed to dissimilation of amyloidogenic vimentin (*pr*Vimentin) that tends to make it resilient against environmental stresses seemingly by self-clearance of coacervates.

Finally we tried to delineate the scenario behind tumor regression found in the Pritumumab therapy against brain tumors by shedding a light on the relationship between prionogenesis of vimentin and the dichotomy of cancer stem cells. The one of the authors in this report advocated praxis of the dichotomous aspect of cancer stem cells [40]. Tumors are initiated from normal stem cells (NSCs) inappropriately affected by tumor micro-environmental niche cells (T-niche). Cancer stem cells (CSCs) abiding in T-niche have the potential to become malignant cells. Non-cancer stem cells occupying T-niche are called differentiated tumor cells. CSC and NSC are reciprocally participating in EMT/MET when CSCs provoke malignant traits such as metastasis, invasion and anti-apoptosis. Prions are required for the stemness of a cell [60]. Stemness genes such as NANOG, SOX2, and OCT4 were expressed aberrantly in CSC yielding aberrant EMT [61]. How does *pr*Vimentin contribute to cancer stem cell maintenance? During EMT induced by anti-apoptosis, the cell is trying to find out the right way to adapt to the new environment via RNA splicing diversity that depends on the function of prion-like ribonucleoproteins / RNA binding proteins [8]. When *pr*Vimentin was resiled to *nr*Vimentin's configuration by virtue of *chap*CLN-IgG destabilizing oncogenic 14-3-3 $\gamma/\epsilon$

by replacing soncogenic 14-3-3 $\sigma$ , it is a prognostic sign that the host is recuperating from malignancy by conversion from aberrant EMT to normalized MET, which brings about the capacity for appropriate apoptosis. This important conversion of EMT to MET is a hallmark for the reprogramming of malignant cells to normal organogenesis. We tried to find the mechanisms for the dichotomy of CSC traits [62] in the conversion of *pr*Vimentin to *nr*Vimentin and vice versa. This could account for phenomena related to CSC reprogramming in 1) the reversion of EMT to MET found in the suppression of vimentin in prostate tumors with attenuated tumor growth and leading to prolonged life span [63], 2) the maintenance of CSC with SOX2 expression was regulated by the suppression of vimentin in glioblastoma [64], and 3) Hsa-miR520-d induced CSCs including glioblastomas in normal tissue via stemness mediated processes [9].

In conclusion the repetitive administration of CLN-IgG (Pritumumab) to brain tumor seems to be a potent modality to control malignancy by virtue of its intervention on the prionogenicity of vimentin via a prion silencing mechanism possessed by patients' ability to renature prionogenic vimentin by autologous chaperonic antibodies which belong to the idiotope image transmission in the idiotypic antibody networks.

#### Acknowledgments

Authors highly indebted to the researchers and engineers, especially Dr. Y. Aotsuka for the cloning of CLN-IgG and Idio-Abs, Dr. M. Yamada for immunohistochemical stains, Mr. Ono for the generation of Idio-Abs and Dr. S. Hotton for teaching of topographical biology. The fund for all research experiments was supported by the Hagiwara Institute of Health (HIH), Japan. The manuscript was prepared in the HIHIMSA Foundation, USA.

**Conflict of Interest:** No Conflicts

#### References

1. Shi F, Yang L, Kouadir M, et al. The NALP3 inflammasome is involved in neurotoxic prion peptide-induced microglial activation. *J. Neuroinflamm.* 2012; 9: 73.
2. Santos TG, Lopes MH, Martins VR. Targeting prion protein interactions in cancer. *Prion.* 2015; 9: 165-73.
3. Prusiner, SB. *Science.* 1982; 216: 136-44.
4. Castle AR, Gill AC. Physiological functions of the cellular prion protein. *Front. Mol. Biosci.* 2017; 4: 19.
5. Zanata SM, Lopes MH, Mercadante AF, et al. Stress-inducible protein 1 is a cell surface ligand for cellular prion that triggers neuroprotection. *EMBO J.* 2002; 21: 3307-16.
6. Kramczyk N, Meier-Stiegen F, Banys M, et al. Expression of stem cell and epithelial-mesenchymal transition markers in circulating tumor cells of breast cancer patients. *BioMed Res Intl.* 2014; 2014: Article ID 415721.
7. Boreddy SR, Srivastava K. Deguelin suppress pancreatic tumor growth and metastasis by inhibiting epithelial to mesenchymal transition in an orthotopic model. *Oncogene.* 2013; 32: 3980-91.

8. Pradell D, Naro C, Sette C, et al. EMT and stemness: flexible processes turned by alternative splicing in development and cancer progression. *Mol Cancer*. 2017; 16: 8.
9. Tsuno S, Wang X, Shomori K, et al. Hsa-miR-520d induces hepatoma cells to form normal liver tissues via a stemness-mediated process. *Sci Rep*. 2014; 4: 3852.
10. Hagiwara H, Sato GH. Human x human hybridoma producing monoclonal antibody against autologous cervical carcinoma. *Mol Biol Med*. 1983; 1: 245-52.
11. Glassy MC, Handley HH, Hagiwara H, et al. UC729-6, a human lymphoblastoid B-cell line useful for generating antibody-secreting human-human hybridomas. *Proc Natl Acad Sci USA*. 1983; 80: 6327-31.
12. Aotsuka Y & Hagiwara H. Identification of a malignant cell associated antigen recognized by a human monoclonal antibody. *Eur J Cancer Clin Oncol*. 1988; 24: 829-38.
13. Hagiwara H, Aotsuka Y, Yamamoto Y, et al. Determination of the antigen/epitope that is recognized by human monoclonal antibody CLN-IgG. *Hum Antibodies*. 2001; 10: 77-82.
14. Hugwil AV. Antigenicity of the tumor-associated antigen vimentin epitope on ectosomes of brain tumor cell. *Intl J Cancer Res Dev*. 2015; 1: 7-13.
15. Glassy MC, Hagiwara H. Summary analysis of the pre-clinical and clinical results of brain tumor patients treated with pritumumab. *Hum Antibodies*. 2009; 18: 127-37.
16. Hugwil AV, Glassy MC. Idiotypic antibody network regarding malignant cell regression in the brain tumor patients treated with the natural human monoclonal antibody, pritumumab. *Integr. Cancer Biol Res*. 2017; 1: 003.
17. Hagiwara H, Aotsuka Y. Structural analysis of anti-cancer antibody, CLN-IgG, and anti-idiotypic antibody, Idio-No.3, for the study of idiotope image transmission: An insight into antigen-specific human monoclonal antibody therapy, in *Brain Tumor Research and Therapy*, Nagai, M. Ed. (Springer-Verlag, 1996); 371-79.
18. Jerne NK, Roland J, Cazenave PA. Recurrent idiotopes and internal images. *EMBO J*. 1982; 1: 243-47.
19. Masison DC. Perfecting precision of predicting prion propensity. *Proc Natl Acad Sci USA*. 2012; 109: 6362-63.
20. Keeter KM, Stein KC, True HL. Heterologous prion-forming proteins interact to cross-seed aggregation in *saccharomyces cerevisiae*. *Sci Rep*. 2017; 7: 5853.
21. Eulitz M, Weiss DT, Solomon A. Immunoglobulin heavy-chain-associated amyloidosis. *Proc Natl Acad Sci USA*. 1990; 87: 6542-46.
22. Foote M, Zhou Y. 14-3-3 proteins in neurological disorders. *Intl. Biochem. Mol Biol*. 2012; 3: 152-64.
23. Shimada T, Fournier A, Yamagata K. Neuroprotective function of 14-3-3 proteins in neurodegeneration. *BioMed Res Intl*. 2013; 564534.
24. Ostreterova N, Petrucelli L, Farrer M, et al.  $\alpha$ -Synuclein shares physical and functional homology with 14-3-3 proteins. *J Neurosci*. 1999; 19: 5782-91.
25. Moussaud S, Jones D, Maussaud-Lamodièrre EL, et al. Alpha-synuclein and tau: teammates in neurodegeneration? *Mol Neurodegen*. 2014; 9: 43.
26. Fede GD, Giaccone G, Limido L, et al. The  $\epsilon$  isoform of 14-3-3 protein is a component of the prion protein amyloid deposits of Gerstmann-Sträussler-Scheinker disease. *J Neuropath Exp Neurol*. 2007; 66: 124-30.
27. Titani K, Shinoda T, Putnam FW. The amino acid sequence of a  $\kappa$  type Bence-Jones protein. *J Biol Chem*. 1969; 244: 3550-60.
28. Jia B, Wu Y, Zhou Y. 14-3-3 and aggresome formation implications in neurodegenerative diseases. *Prion*. 2014; 8: 173-77.
29. Ackbarow T, Buehler MJ. Molecular mechanics of stutter defects in vimentin intermediate filaments. *Exp. Mechanics*. 2009; 49: 79-89.
30. Arslan M, Qin Z, Buehler MJ. Coiled-coil intermediate filament stutter instability and molecular unfolding. *J Compu Meth Biomec Biomed Eng*. 2011; 14: 483-89.
31. Chen W, Hu Z, Li XZ, et al. CPEB4 interacts with vimentin and involves in progressive features and poor prognosis of patients with astrocytic tumors. *Tumor Biol*. 2016; 37: 5075-87.
32. Lu R, Zhou Z, Yu W, et al. CPEB4 promotes cell migration and invasion via upregulating vimentin expression in breast cancer. *Biochem. Biophys. Res. Commu*. 2017; 489: 135-41.
33. Ozawa D, Nomura R, Mangione PP, et al. Multifaced anti-amyloidogenic and pro-amyloidogenic effects of C-reactive protein and serum amyloid P component in vitro. *Sci Rep*. 2016; 6: 29077.
34. Tong J, Ang LC, Williams B, et al. Low levels of astroglia markers in Parkinson Disease: relationship to  $\alpha$ -synuclein accumulation. *Neurobiol Dis*. 2015; 82: 243-53.
35. Johnston JA, Ward CL, Kopito RR. Aggresomes: A cellular response to misfolded proteins. *J Cell Bio*. 1998; 143: 1883-98.
36. Ogrodnik M, Salmonowicz H, Brown R, et al. Dynamic JUNQ inclusion bodies are asymmetrically inherited in mammalian cell lines through the asymmetric partitioning of vimentin. *Proc Natl Acad Sci USA*. 2014; 111: 8049-54.
37. Bauer PO, Huadec R, Goswami A, et al. ROCK-phosphorylated vimentin modifies mutant huntingtin aggregation via sequestration of IRBIT. *Mol Neurodegen*. 2012; 7: 43.
38. Levin EC, Acharya NK, Sedeyn JC, et al. Neuronal expression of vimentin in Alzheimer's disease brain may be part of a generalized dendritic damage-response mechanism. *Brain Res*. 2009; 1298: 194-207.
39. Pére-Sala D, Oeste CL, Martinez AE, et al. Vimentin filament organization and stress sensing depend on its single cystein residue and zink binding. *Nat Commu*. 2015; 6: 7287.
40. Hugwil AV. The meaning of the anti-cancer antibody CLN-IgG (Pritumumab) generated by human x human hybridoma technology against the cyto-skeletal protein, vimentin, in the course of the treatment of malignancy. *Med Hypotheses*. 2013; 81: 489-95.
41. Nunziante M, Ackermann, K, Dietrich K, et al. Proteasomal dysfunction and endoplasmic reticulum stress enhance trafficking of prion protein aggregates through the secretory pathway and increase accumulation of pathologic prion proteins. *J Biol Chem*. 2011; 286: 33942-953.
42. Clapp C, Portt L, Khoury C, et al. 14-3-3 protects against stress induced apoptosis. *Cell Death Dis*. 2012; 3: e348.
43. Bechtold DA, Brown IR. Induction of Hsp27 and Hsp32 stress proteins and vimentin in glial cells of the rat hippocampus following hyperthermia. *Neurochem. Res*. 2003; 28: 1163-74.
44. Kong Q, Xie B, Li J, et al. Identification and chracterization of an oocyte factor required for porcine nuclear reprogramming. *J Biol Chem*. 2014; 289: 6960-68.
45. Boraas L, Ahsan T. Lack of vimentin impairs endothelial differentiation of embryonic stem cells. *Sci. Rep*. 2016; 6: 30814.
46. Sato R, Semba T, Saya H, et al. Stem cells and epithelial-mesenchymal-transition in cancer: biological implications and therapeutic targets. *Stem Cells*. 2016; 34: 1997-2007.
47. Chang TC, Liu CC, Hsing EW, et al. 14-3-3 $\sigma$  regulates  $\beta$ -catenin mediated mouse embryonic stem cell proliferation by sequestering GSK-3 $\beta$ . *PLoS ONE*. 2012; 7: e40193.
48. Mackintosh C. Dynamic interactions between 14-3-3 proteins and phosphoproteins regulate diverse cellular processes. *Biochem. J*. 2004; 381: 329-42.
49. Oparin AI. *The origin of life* (Dover Pub Inc. NY 1953). 137-62
50. Blocher WC, Perry SL. Complex coacervate-based materials for biomedicine. *Wiley Interdiscip. Nanomed. Nanotechnol*. 2017; 9: e1442.
51. Aumiller Jr WM, Keating CD. Experimental models for dynamic compartmentalization of biomolecules in liquid organelles: reversible formation and partitioning in aqueous biphasic systems. *Adv Colloid Inter Sci*. 2017; 239: 75-87.
52. Rostami J, Holmqvist S, Lindström V, et al. Human astrocytes transfer aggregated alpha-synuclein via tunneling nanotubes. *J. Neurosci*. 2017; 37: 11835-853.
53. Ady JW, Pesir S, Thayanithy V, et al. Intercellular communication in

- malignant pleural mesothelioma: properties of tunneling nanotubes. *Front Physiol.* 2014; 5: 400.
54. Williams DM, Ecroyd H, Goodwin KL, et al. NMR spectroscopy of 14-3-3  $\zeta$  reveals a flexible C-terminal extension: differentiation of the chaperone and phosphoserine-binding activities of 14-3-3  $\zeta$ . *Biochem. J.* 2011; 473: 493-503.
  55. Muslin AJ, Tanner JW, Allen PM, et al. Interaction of 14-3-3 with signaling proteins is mediated by the recognition of phosphoserine. *Cell.* 1996; 84: 889-97.
  56. Lee YS, Lee JK, Bae Y, et al. Suppression of 14-3-3 $\gamma$ -mediated surface expression of ANO1 inhibits cancer progression of glioblastoma cells. *Sci Rep.* 2016; 6: 26413.
  57. Yang HY, Wen YY, Chen CH, et al. 14-3-3 $\sigma$  positively regulates p53 and suppresses tumor growth. *Mol Cell Biol.* 2003; 23: 7096-107.
  58. Liu TA, Jan YJ, Ko BS, et al. 14-3-3 $\epsilon$  overexpression contributes to epithelial-mesenchymal transition of hepatocellular carcinoma. *PLoS ONE.* 2013; 8: e57968.
  59. Cohen E, Taraboulos A. Scrapie-like prion protein accumulates in aggregates of cyclosporin A-treated cells. *EMBO J.* 2003; 22: 404-17.
  60. Zhang CC, Steele AD, Lindquist S, et al. Prion protein is expressed on long-term repopulating hematopoietic stem cells and is important for their self-renewal. *Proc. Natl. Acad. Sci. USA.* 2006; 103: 2184-89.
  61. Gawlik-Rzemieniewska N, Bednarek I. The role of NANOG transcriptional factor in the development of malignant phenotype of cancer cells. *Cancer Biol Ther.* 2016; 17: 1-10.
  62. Hugwil AV. On the dichotomous aspect of cancer stem cell. *J. Cancer Oncol.* 2018; 2: 000123.
  63. Zhang X, Fournier MV, Ware JL, et al. Inhibition of vimentin or  $\beta 1$  integrin reverts morphology of prostate tumor cells grown in laminin-rich extracellular matrix gels and reduces tumor growth in vivo. *Mol Cancer Ther.* 2009; 8: 499-508.
  64. Deng Z, Du WW, Shan SW, et al. The intermediate filament vimentin mediates microRNA-378 function in cellular self-renewal by regulating the expression of the Sox2 transcription factor. *J Biol Chem.* 2013; 288: 319-31.

To cite this article: Hugwil AV, Glassy MC. Prionogenicity of vimentin surmised from the sequelog of anti-idiotypic antibodies toward the paratope of malignant-associated autologous anti-vimentin antibody, CLN-IgG (Pritumumab). *British Journal of Cancer Research.* 2018; 1:1. doi: 10.31488/bjcr.1000104

© Hugwil AV, et al. 2018.